INTERNATIONAL
Agrophysics
www.international-agrophysics.org

Int. Agrophys., 2026, 40, 393-403
doi: 10.31545/intagr/224512

Multifunctional characterisation of novel biocomposite materials**

Ľubomír Kubík[1], *Maja Karaman*[2], *Monika Božiková*[1]*, *Vladimír Madola*[3], *Nenad Krsmanović*[4], *Milivoj Radojčin*[5], *Siniša Bikić*[5], *Peter Hlaváč*[1]

[1]Institute of Electrical Engineering, Automation, Informatics and Physics, Slovak University of Agriculture in Nitra, Tr. A. Hlinku 2, SK-949 76 Nitra, Slovakia
[2]Department of Biology and Ecology, University of Novi Sad, Trg Dositeja Obradovića 2, RS-21000 Novi Sad, Serbia
[3]Information and Coordination Centre of Research, Slovak University of Agriculture in Nitra, Tr. A. Hlinku 2, SK-949 76 Nitra, Slovakia
[4]Mycotopia R&D Company, Lekina 37, RS-222 32 Divoš, Sremska Mitrovica, Serbia
[5]Department of Agricultural Engineering, University of Novi Sad, Trg Dositeja Obradovića 2, RS-21000 Novi Sad, Serbia

Received February 22, 2026; accepted June 12, 2026

A b s t r a c t. The article presents a multifunctional characterisation of biocomposite materials through the systematic determination of physical properties. Two specimens were synthesised: a substrate comprising 100% straw (density 326.57±33.29 kg m^{-3}) and the other composed of 70% straw and 30% sawdust (density 190.94±12.87 kg m^{-3}) with the mycelium of a *Schizophyllum commune* Fr. 1815 strain. Mechanical characterisation revealed differential modulus values ranging from 166.75 to 587.87 kPa, with enhanced formulation demonstrating a 3.65-fold improvement, achieving 1 541.40 kPa (R^2 = 0.96-0.98). Thermal property evaluation employed the plane source methodology with uncertainties below 5%. Both specimens exhibited exceptional thermal insulation with conductivity coefficients of 0.0477±0.0008 and 0.0480±0.0011 W m^{-1} K^{-1}. Statistical analysis confirmed no significant difference (t = 0.3870, p = 0.7046), with variation coefficients of 1.57 and 2.34%. Thermal diffusivity reached 0.128±0.0043 × 10^{-6} m² s^{-1} and 0.130±0.0042 10^{-6} m² s^{-1} (p = 0.7404). Electrical characterisation across 40 to 110 MHz revealed frequency-dependent transitions with exponential correlations (R^2 = 93.64 and 95.50%). Sample B demonstrated inductive characteristics up to 95.15 MHz transition frequency. Pearson correlation analysis established a strong negative correlation for sample A (r = -0.8361, p < 0.0001) versus a moderate positive correlation for sample B (r = 0.2461, p = 0.0004). These findings establish quantitative structure-property relationships fundamental to multifunctional engineering applications.

K e y w o r d s: biocomposite, mechanical properties, thermal parameters, electrical characteristics, innovative material

1. INTRODUCTION

Biocomposite materials represent a significant advancement in contemporary materials science, constituting the synergistic integration of natural fibres within polymer matrices to achieve a confluence of environmental sustainability and engineering functionality (Ahmadi *et al*., 2025; Chen *et al*., 2023). These materials embody the transition from conventional synthetic composites towards bio-based alternatives, fundamentally addressing the imperative for renewable resource utilisation whilst maintaining requisite mechanical performance characteristics for advanced engineering applications (Hamdi *et al*., 2024; Khouaja *et al*., 2025). Mycelium-based biomaterials provide a sustainable solution by converting lignocellulosic waste into biodegradable, fully bio-based composites suitable for packaging and construction applications. Most mycelium-based materials are grown on agricultural waste materials; the most commonly used are white-rot fungi from the genera

*Corresponding author e-mail: Monika.Bozikova@uniag.sk
**This work was prepared within the framework of the project VEGA No. 1/0221/25. The usage of artificial intelligence to optimize the conditions of biomass thermochemical conversion and by the project Drive4SIFood 313011V336, cofinanced by the European Regional Development Fund and SUA Grant Agency – research project No. 15-GA-SPU-2024.

Ganoderma, *Pleurotus*, and *Trametes*. *S. commune*, commonly known as the "two-leaf" mushroom, is a widespread pathogen that attacks living and injured plant tissue and is also an aggressive invader of trees, causing a disease classified as white rot (Takemoto *et al.*, 2010). The species *S. commune* rapidly colonises more than 260 species from 150 plant genera (Cooke, 1961) through lesions caused by other pathogens. Mycelium-based materials are renewable and recyclable and can replace, among others, various plastics. A mycelium-based material is a composite consisting of a natural reinforcement or filler, such as hemp fibres, and fungal mycelium. The mycelium is a dense network of thin strands called hyphae that grow and fuse together into a solid material. The mycelium acts as a three-dimensional matrix that binds the natural substrate into a lightweight material, comparable to expanded polystyrene.

The technological evolution of biocomposite systems has progressed substantially from primitive applications utilising natural reinforcements in traditional construction materials to sophisticated engineered composites incorporating contemporary fibre modification methodologies and advanced interfacial optimisation strategies (Yadav *et al.*, 2022). Modern biocomposite technologies facilitate the development of materials exhibiting mechanical properties comparable to synthetic analogues whilst maintaining inherent biodegradability and substantially reduced environmental impact profiles (Paulsingarayar *et al.*, 2025; Suherman *et al.*, 2024).

Contemporary research in biocomposite characterisation encompasses comprehensive multidisciplinary evaluation of mechanical, thermal, and electrical properties, with particular emphasis on elucidating fibre-matrix interfacial phenomena and optimising adhesion mechanisms through advanced surface treatment methodologies (Chougala *et al.*, 2025; Shen *et al.*, 2024). Current investigations systematically address the inherent limitations of natural fibres, specifically their hydrophilic characteristics and consequent incompatibility with hydrophobic polymer matrices, through implementation of sophisticated chemical and biological treatment protocols (Saada *et al.*, 2024).

Mechanical characterisation of biocomposite systems employs advanced testing methodologies, including the evaluation of strain-dependent mechanical behaviour through compression testing with differential modulus analysis. These investigations reveal complex viscoelastic responses characterised by frequency-dependent storage and loss moduli, with differential modulus values demonstrating strain-dependent behaviour patterns and enhancement factors exceeding 3.5 in optimally formulated systems (Paulsingarayar *et al.*, 2025). Contemporary mechanical evaluation encompasses tensile, flexural, and impact resistance assessments, with systematic investigation of interfacial shear strength properties to establish structure–property relationships (Chougala *et al.*, 2025).

Thermal property characterisation represents a critical research domain encompassing precise measurement of thermal conductivity, thermal diffusivity, and specific heat capacity utilising dynamic plane source methodologies (Božiková *et al.*, 2021; Bojković N. *et al.*, 2023). Recent investigations employing transient plane source techniques have achieved measurement uncertainties below 5% for thermal conductivities ranging from 0.01 to 2 W m^{-1} K^{-1}, demonstrating exceptional thermal insulation properties competitive with those of conventional building materials (Mizera *et al.*, 2017). Systematic thermal analyses reveal thermal conductivity values ranging from 0.048 to 0.27 W m^{-1} K^{-1} for various biocomposite formulations, substantially outperforming traditional materials including wood and concrete in insulation applications (Chen *et al.*, 2023; Zine *et al.*, 2023).

Electrical characterisation through impedance spectroscopy represents an emerging research frontier providing fundamental insights into ionic conductivity mechanisms, interfacial polarisation phenomena, and frequency-dependent dielectric relaxation processes (Pramono *et al.*, 2017; Zhang W. *et al.*, 2022). Contemporary investigations employ precision impedance analysis across extended frequency ranges of 40 to 110 MHz, revealing characteristic frequency-dependent transitions from inductive to capacitive behaviour and establishing quantitative structure-property relationships essential for applications in biosensor technologies and biodegradable electronics (Kirubakaran *et al.*, 2024). Since research on the mechanical performance of mycelium-based materials is very limited, the principal objective of this investigation encompasses comprehensive multifunctional characterisation of biocomposite materials through the evaluation of integrated mechanical, thermal, and electrical property, establishing quantitative correlations between microstructural features and macroscopic performance characteristics.

The research pursues three fundamental aims: determination of strain-dependent mechanical behaviour through systematic compression testing incorporating differential modulus analysis; precise measurement of thermal transport properties employing the dynamic plane source methodology with rigorous uncertainty quantification; and comprehensive electrical characterisation through impedance spectroscopy across extended frequency ranges with systematic evaluation of frequency-dependent phenomena. The research contribution encompasses simultaneous evaluation of mechanical, thermal, and electrical properties with statistical validation protocols, establishing an extensive property database to inform optimal biocomposite formulation strategies for multifunctional engineering applications.

2. MATERIALS AND METHODS

The samples used in the experiment were obtained by mixing a substrate comprising 100% straw and composed of 70% straw and 30% sawdust with the mycelium of a *Schizophyllum commune* strain from the FCB070 ProFungi Laboratory, Serbia. In both formulations, the mycelium served as a natural bio-based binder that integrated lignocellulosic particles into a coherent composite structure. The reference material (sample A Fig. 1a) consisted of 100% straw, whereas the modified material (sample B Fig. 1b) consisted of 70 straw and 30% sawdust.

The moisture content and temperature conditions used during biocomposite fabrication were selected to ensure reproducible mycelial growth and structurally stable composites. The lignocellulosic substrate was adjusted to a moisture content from 59.6 to 72.5% (wet basis), providing sufficient water availability for fungal colonisation while avoiding the formation of free-water zones detrimental to aerobic growth. The inoculated substrates were incubated under controlled mesophilic conditions at 21.5-23.4°C, followed by post-growth drying at 40-60°C to terminate biological activity and stabilise the mechanical, thermal, and electrical properties of the mycelium-based composites. Prior to inoculation, the substrates were homogenised to obtain a uniform distribution of the lignocellulosic fraction and fungal inoculum. The inoculated material was then placed into moulds of defined geometry, where the samples were formed during mycelial growth. No additional synthetic binder was used during sample preparation.

For the determination of biocomposite sample densities, dimensional characteristics were measured 5 times for each sample using vernier callipers (Nónius, Hoffmann GmbH, Germany) with an accuracy of ±0.05 mm. The specimens' masses were determined using Kern analytical scales (Kern and Sohn GmbH, Germany) with an accuracy of ±0.01 g. Volumetric density was calculated as the ratio of mass and volume of the sample. Density values of 326.57±33.29 kg m^{-3} for the mould-additive sample B and 190.94±12.87 kg m^{-3} for the reference sample A were obtained, thereby enabling subsequent quantitative assessment of the mould additive's influence on the physical properties of the biocomposite.

In mycelium-based composites, the final material properties are strongly affected by the substrate composition, particle size, growth environment, and post-growth treatment; therefore, these parameters should be stated explicitly for reproducibility. Prior to inoculation, the substrates were homogenised and conditioned to the required moisture content, because water availability and nutrient balance directly influence fungal colonisation and the integrity of the mycelial binding network (Houette *et al.*, 2022; Elsacker *et al.*, 2020). The inoculated substrate was then placed into moulds of defined geometry and incubated under controlled conditions until complete colonisation was visually confirmed. After the growth stage, the samples were dried to stop further biological activity and stabilise the material structure before testing (Jiménez-Obando *et al.*, 2025).

The mechanical properties of two biocomposite materials were evaluated through compression testing using a custom-built testing apparatus developed at the Faculty of Engineering (Slovak University of Agriculture in Nitra, Slovakia). The testing system consisted of a force sensor with a maximum capacity of 1 000 N and an accuracy of ±0.4%, coupled with a displacement sensor exhibiting ±1% accuracy. All compression tests were conducted at a constant loading rate of 10 mm min^{-1}. Four specimens from each biocomposite material were prepared by cutting into prismatic shapes for mechanical evaluation.

The compression testing was performed using a parallel-plate configuration, where samples were positioned between two metal plates, with the upper loading plate featuring a circular geometry of 79 mm diameter to ensure uniform stress distribution across the specimen surface. Compression loading was applied incrementally until the onset of visible material damage, characterised by localised failure at the contact interface between the specimen and the metal loading plate. Due to sensor limitations, the maximum applied force was restricted to approximately 800 N to prevent sensory overload. Force-displacement curves were recorded throughout the testing process, from which stress-strain relationships and the elastic module were subsequently calculated.

a)

b)

Fig. 1. Structure depiction of material: a) biocomposite sample A and b) biocomposite sample B.

Compression loading was applied within the safe operating limit of the testing system, and the maximum load was restricted to approximately 800 N to prevent sensor overload. Therefore, the endpoint of the test should be interpreted as the maximum accessible loading window of the apparatus and/or the onset of visible local damage, rather than unequivocal catastrophic failure of all specimens. This distinction is important because mycelium-based composites often exhibit progressive densification and may not fail abruptly within the selected loading interval (Houette *et al.*, 2022). Compressive stress σ defined by (Eq. (1)) was calculated as the ratio of applied force F to the cross-sectional area of the specimen S, expressed as:

$$\sigma = \frac{F}{S}, \tag{1}$$

where: σ represents compressive stress (Pa), F denotes applied force (N), and S indicates the cross-sectional area (mm^2). Compressive strain ε was determined from the dimensional changes during loading according to Eq. (2):

$$\varepsilon = \frac{\Delta l}{l_0}, \tag{2}$$

where: ε represents compressive strain (mm mm^{-1}), Δl denotes specimen shortening (mm), and l_0 indicates the original specimen height (mm). The elastic modulus was derived from the linear portion of the stress-strain relationship according to Hooke's law, expressed by Eq. (3):

$$\sigma = E\varepsilon + a, \tag{3}$$

where: E represents Young's modulus of elasticity (Pa) and a denotes the regression coefficient (Pa). The elastic modulus E was determined as the slope of the linear regression line fitted to the stress-strain data in the elastic deformation region.

Four specimens per passage were tested mechanically; therefore, the mechanical dataset should be considered exploratory. Although the average trends are informative, the low number of replicates limits the power of formal statistical inference between formulations. Previous studies on mycelium-based composites commonly emphasise the strong sensitivity of compressive properties to density, substrate architecture, and post-processing, which further supports the need for larger test sets in future studies (Jiménez-Obando *et al.*, 2025). Therefore, the present mechanical results are interpreted primarily as comparative trends rather than definitive population-level values.

Thermal parameters were investigated by the dynamic plane source (DPS) method, as presented in ISO 22007-2, which utilises a planar double-spiral nickel sensor that serves as both an electric heater and a resistance thermometer simultaneously. The dimensions of the thermal-test specimens were 65 × 65 × 12 mm. Before measurement, the samples were conditioned in the dried and stabilised state obtained after the post-growth treatment described above. The thermal measurements were carried out under laboratory temperature conditions corresponding to the measuring environment used for the DPS analysis. When a constant current passes through the sensor, an instantaneous areal heat flux q_0 is generated, and the resulting transient temperature field in the two identical half-spaces of the specimen is described by the heat-conduction Eq. (4):

$$\frac{\partial T}{\partial t} = a\nabla^2 T + \frac{q_0}{c\rho\delta(r)\delta(t)}, \tag{4}$$

where: a – thermal diffusivity (m^2 s^{-1}), T – absolute temperature (K), t – time (s), $c\rho$ – volume heat capacity (W m^{-3} K^{-1}), r – distance from the heat source (m)

For the dimensionless time parameter $\tau = at/r_s^2$ restricted to the fitting window $0.5<\tau<2$, the mean temperature rise of the sensor $\Delta T(t)$ is defined by Eq. (5):

$$\Delta T(t) = \frac{q_0}{\pi^{\frac{3}{2}}\lambda r_S\sqrt{t}} G(\tau), \tag{5}$$

where: λ – is thermal conductivity (W m^{-1} K^{-1}), r_S – is the mean radius of the outermost spiral of the probe, and $G(\tau)$ is Green´s function factor.

The result of measuring thermophysical parameters is influenced by several factors, the effect of which can be corrected by the following means: To minimise finite-geometry errors, the thermal penetration depth $\delta = \sqrt{\pi a t}$ must remain below 70% of the specimen's half-thickness throughout the selected measurement time window. The surface source is placed between two flat, parallel specimen halves and clamped with a normal force of approximately 25 N to minimise thermal contact resistance. The sensor's voltage response, corresponding to a self-heating of less than 5°C, is digitised with a resolution better than 1 mK and processed by software. If the specified experimental conditions are met, the measurement uncertainty of this method remains below 5% for thermal conductivities in the range of 0.01-2 W m^{-1} K^{-1}.

Measurement methodology for electrical characterisation of biocomposites – the electrical properties of the biocomposites were characterised through impedance spectroscopy, focusing on the complex impedance Z (Eq. (6)) and the phase angle φ. Measurements were performed using a precision impedance analyser (Agilent 4294A) in a four-terminal-pair (4TP) configuration to minimise lead resistance and stray capacitance effects. The frequency range was set from 40 to 110 MHz with a logarithmic sweep of 10 points per decade to capture both interfacial polarisation and bulk dielectric responses:

$$Z = |Z|e^{j\Phi}. \tag{6}$$

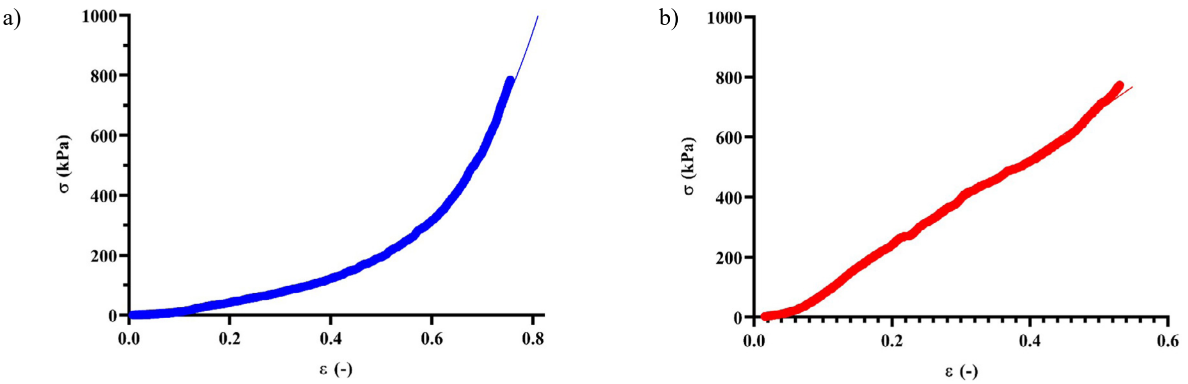

Fig. 2. Relation between compressive stress and deformation for: a) sample A and b) sample B.

A small AC excitation signal (1 V amplitude) was applied to ensure linear material response while avoiding electrochemical degradation at the electrode-sample interface. The phase angle resolution was maintained at a value of ±0.1° through internal phase-locked loop synchronisation and instrument warm-up stabilisation.

Impedance *Z* is a complex quantity defined by Eq. (7) as:

$$Z = Z' + j\,Z'', \tag{7}$$

where: *Z*' represents the real part of impedance (Ω) and *Z*'' is the imaginary part of impedance (Ω), reflecting the material's ability to resist and store electrical energy, respectively. In biocomposites, impedance analysis reveals critical insights into ionic conductivity, interfacial polarisation, and dielectric relaxation, which are influenced by the material's microstructure and hydration state. Understanding these properties is crucial for applications such as biosensors, tissue engineering scaffolds, and biodegradable electronics, where electrical interactions with biological systems significantly impact functionality and performance. Additionally, the frequency-dependent impedance response helps distinguish between bulk material properties and electrode effects, enabling optimisation of composite formulations for specific biomedical or energy storage applications.

3. RESULTS AND DISCUSSION

The selected mechanical, thermal, and electrical properties of biocomposite materials were evaluated to characterise their multifunctional performance and establish structure-property relationships for potential engineering applications.

3.1. Mechanical properties of biocomposite materials under compression loading

The compression testing of the biocomposite specimens revealed distinct viscoelastic behaviour with progressive deformation phases and strain-dependent elastic moduli. The loading diagram presented in Fig. 2a demonstrates the stress-strain relationship for the 3-point biocomposite material, calculated as the average response from four identical specimens. Compression testing was conducted over a deformation range of 0-75%.The loading diagram presented in Fig. 2b demonstrates the stress-strain relationship for the 3-biocomposite material, calculated as the average response from four identical specimens. Compression testing was conducted over a deformation range of 0-54%. The compression response of both mycelium-based composites exhibited a strain-dependent behaviour typical of porous bio-based cellular materials. At low deformation, the response was associated with initial rearrangement of the internal porous structure, whereas at higher strain levels, progressive densification contributed to the increase in apparent stiffness.

Deformation behaviour and elastic response – the mechanical response exhibited three distinct phases during compression loading. Initially, elastic deformation was observed up to approximately 10% strain, followed by a transition to viscoelastic and plastic deformation regimes at higher strain levels. This behaviour is consistent with biocomposite materials, where different deformation mechanisms become activated at increasing stress levels.

The differential modulus of elasticity was determined from the linear portions of the loading curves according to Young's law of elasticity, calculated as the slope of the tangent to the differential sections of the stress-strain curves. This approach provides more accurate representation of the material's stiffness characteristics across different strain ranges compared to conventional secant modulus calculations. In our case, the experimental dependence can be described by the exponential nonlinear function (Eq. (8)) with a coefficient of determination of R^2 = 0.9969 and RMSE = 10.57 kPa (Fig. 2a):

$$\sigma = 13.49\ e^{5{,}314\,\varepsilon}. \tag{8}$$

Figure 2b presents the loading diagram, which can be characterised by Eq. (9). The coefficient of determination was R^2 = 0.9970 and RMSE = 12.33 kPa:

$$\sigma = 190.2\,\varepsilon^2 + 1384\,\varepsilon - 49.23. \tag{9}$$

3.1.1. Strain-dependent elastic modulus

Table 1 presents the differential modulus values for the 3-point biocomposite at various deformation ranges. The modulus values demonstrated significant strain dependence, ranging from 166.75 kPa at low strains (0-10%) to 587.87 kPa at intermediate strains (30-50%).

The accuracy of the differential modulus determination was consistently high, with measurement uncertainties ranging from 0.15 to 2.00%, indicating excellent repeatability and reliability.

Comparative analysis with the enhanced 3-biocomposite material revealed substantially improved mechanical properties, with differential modulus values approximately 3.65 times higher across all tested strain ranges (Table 2). The 3-biocomposite exhibited modulus values ranging from 851.42 kPa (0-10% strain) to 1 541.4 kPa (10-30% strain).

The strain-dependent modulus behaviour reflects the complex microstructural response of biocomposite materials under compression. At low strain levels, the relatively low modulus values indicate initial matrix-dominated deformation, where the polymer matrix accommodates applied stress through elastic deformation mechanisms (Bodur and Bakkal, 2019). The progressive modulus increase suggests enhanced load transfer to the reinforcing phase as the matrix approaches its elastic limits.

Table 1. Differential modulus of elasticity for 3-point biocomposite material

Deformation range (%)	Differential modulus (kPa)	R^2 (-)
0-10	166.75	>0.98
10-30	319.54	>0.98
30-50	587.87	>0.98
0-50	379.35	>0.96

Table 2. Comparative differential modulus of elasticity

Deformation range (%)	3-point (kPa)	3-biocomposite (kPa)	Enhancement factor (-)
0-10	166.75	851.42	5.10
10-30	319.54	1541.40	4.82
30-50	587.87	1422.10	2.42
0-50	379.35	1487.50	3.92

This behaviour is characteristic of natural fibre-reinforced biocomposites, where mechanical response is governed by matrix properties and fibre-matrix interface characteristics. The differential modulus approach provides valuable insights into these progressive deformation mechanisms (Combrzyński *et al*., 2016).

The compression response of both mycelium-based composites exhibited a strain-dependent behaviour typical of porous bio-based cellular materials. At low deformation, the response was associated with initial rearrangement of the internal porous structure, whereas at higher strain levels, progressive densification contributed to the increase in apparent stiffness.

The approximately 3.65-fold increase in differential modulus observed for sample B should be interpreted as an experimentally observed difference between the two tested formulations. A plausible explanation is that the presence of sawdust modified particle packing, local density distribution, and stress transfer through the mycelium-bound structure (Al-Bahadly, 2019).

The viscoelastic nature of both materials, evidenced by the progressive transition from elastic to plastic deformation beyond 10% strain, aligns with theoretical predictions for hierarchically structured biological materials (Kochańska and Bajer, 2012). This behaviour provides advantageous properties for applications requiring energy absorption and damage tolerance (Senthilkumar *et al*., 2022).

The high coefficient of determination values (R^2>0.96) confirms the validity of the linear regression approach, essential for the reliable characterisation of the mechanical properties of biocomposite materials.

3.2. Thermal parameter results

The thermal conductivity measurements revealed stable and consistent values for both biocomposite samples under investigation. Sample A exhibited a mean thermal conductivity of 0.0477 W m^{-1} K^{-1} with a standard deviation of 0.000751 W m^{-1} K^{-1}, while Sample B demonstrated a mean value of 0.0480 W m^{-1} K^{-1} with a standard deviation of 0.00112 W m^{-1} K^{-1}. The coefficients of variation were 1.57 and 2.34% for Samples A and B, respectively, indicating excellent measurement reproducibility, with Sample A exhibiting superior precision. Statistical analysis using an unpaired t-test confirmed no significant difference between the thermal conductivity values of the two samples (t = 0.3870, df = 14, p = 0.7046). The F-test demonstrated homogeneous variances (F = 2.227, p = 0.2802), further supporting the statistical equivalence of both samples. This consistency suggests robust manufacturing processes, which are critical for potential commercial applications (Brzyski *et al*., 2017).

The measured thermal conductivity values demonstrate excellent thermal insulation properties consistent with high-performance natural fibre composites reported in recent literature (Neto *et al*., 2021). These values substantially

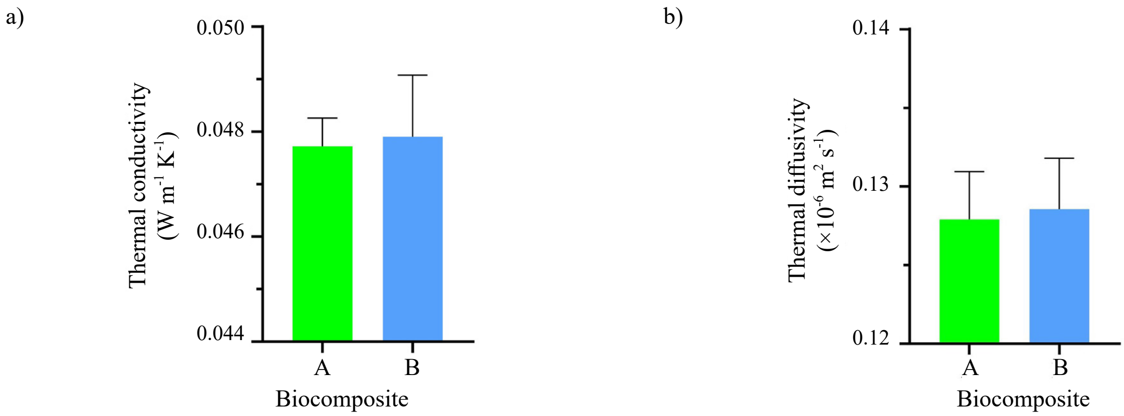

Fig. 3. Thermal conductivity (a) and thermal diffusivity (b) of biocomposite samples with 95% confidence intervals.

exceed the performance of conventional building materials, which typically exhibit thermal conductivities ranging from 0.13 W m^{-1} K^{-1} for wood to 2.3 W m^{-1} K^{-1} for concrete (Bojković J. *et al*., 2023). When compared to other natural fibre insulation materials investigated in recent studies, which reported thermal conductivity values between 0.0333 and 0.0438 W m^{-1} K^{-1} (Mawardi *et al*., 2021), the present biocomposite samples demonstrate competitive thermal insulation performance. The statistical equivalence between the samples (Fig. 3) indicates the reliability of the production methodology and suggests promising potential for consistent commercial-scale manufacturing.

The very small difference in thermal conductivity between samples A and B (Fig. 3a) suggests that the partial replacement of straw by sawdust did not substantially modify the dominant heat-transfer pathways within the tested density range. This is consistent with literature indicating that thermal transport in mycelium-based composites is governed primarily by overall porosity, density, and internal air volume (Wildman *et al*., 2026).

The thermal diffusivity measurements demonstrated consistent behaviour across both biocomposite samples under investigation. Sample A exhibited a mean thermal diffusivity of 0.128 10^{-6} m^2 s^{-1} with a standard deviation of 0.00425 10^{-6} m^2 s^{-1}, while Sample B demonstrated a mean value of 0.130 10^{-6} m^2 s^{-1} with a standard deviation of 0.00422 10^{-6} m^2 s^{-1} (Fig. 3b). Both samples exhibited identical measurement ranges of 0.0130 10^{-6} m^2 s^{-1}, and the nearly identical standard deviations indicate comparable material uniformity throughout the composite structure. Statistical analysis using an unpaired t-test confirmed no statistically significant difference between the thermal diffusivity values of the two samples (t = 0.3368, df = 17, p = 0.7404). The F-test analysis validated variance homogeneity between the samples (F=1.018, p = 0.9907), further supporting the statistical equivalence and demonstrating excellent measurement precision with low coefficients of variation.

The measured thermal diffusivity values indicate efficient heat transfer characteristics within the biocomposite microstructure, representing the rate of temperature change propagation through the material matrix (Parker *et al*., 1961). These measurements fall within the typical range reported for wood-based materials, which commonly exhibit thermal diffusivity values between 0.08 and 0.143 10^{-6} m^2 s^{-1}.

According to established literature, thermal diffusivity in natural fibre composites is significantly influenced by fibre orientation and matrix-fibre interface properties (Abbas *et al*., 2020). The low coefficient of variation observed in both samples validates the measurement precision and confirms material uniformity across the composite structure (Zhang L. *et al*., 2022). The statistical equivalence between the samples suggests consistent microstructural characteristics and reinforces the reliability of the manufacturing process for achieving reproducible thermal transport properties.

3.3. Impedance analysis results

The impedance measurements revealed distinct frequency-dependent electrical characteristics for both biocomposite samples A and B. The relationships between impedance Z and frequency f are exponential functions for both biocomposite samples (Fig. 4).

The regression curve of impedance A is represented by Eq. (10), where R^2 was 93.64%:

$$Z = 1.1417\ 10^9 e^{-1.414 \times 10^{-5} f}. \tag{10}$$

The regression curve of impedance B is described by Eq. (11), where R^2 was 95.50%:

$$Z = 0.9916\ 10^9 e^{-1.271 \times 10^{-5} f}. \tag{11}$$

The regression analysis of impedance Z exhibited characteristic patterns that reflect the underlying electrical structure of the biocomposite materials, which is in good agreement with Beltrán-Pitarch *et al*. (2019).

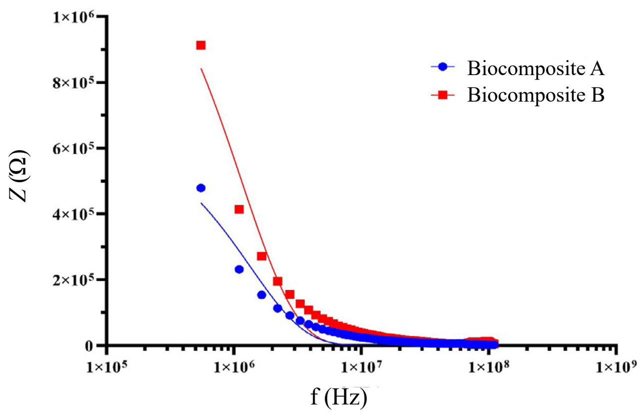

Fig. 4. Nonlinear dependency for impedance values on frequency for samples A and B.

Biocomposite B demonstrated a predominant inductive character in the frequency range from 40 to 95.15 MHz, indicating that the imaginary component of impedance increased proportionally with frequency according to $Z_L = j\omega L$ (Bieńkowski *et al.*, 2023). A notable transition occurred at 95.15-95.70 MHz, where the material character shifted from inductive to capacitive. This frequency-dependent transition is characteristic of biocomposite materials where the balance between conductive and dielectric components changes with applied frequency (Marković *et al.*, 2019). The positive phase-angle region observed for sample B (Fig. 5) is interpreted here as an apparent inductive-type response of the measured specimen-electrode system rather than direct evidence that the biocomposite behaves as a classical inductive component. In heterogeneous bio-based materials, such behaviour may arise from a combination of distributed charge transport pathways, interfacial polarisation, electrode effects, and moisture-dependent ionic conduction, especially at higher frequencies (Mayne *et al.*, 2023). The observed frequency-dependent electrical behaviour suggests possible relevance for future sensing or frequency-responsive bio-based material concepts (Gandia and Adamatzky, 2024).

The capacitive behaviour at higher frequencies follows $Z_C = 1/(j\omega C)$, where impedance decreases with increasing frequency (Dolainski *et al.*, 2024). This transition indicates that dielectric properties dominate over conductive characteristics at higher frequencies, resulting in energy storage rather than energy dissipation (Fig. 4).

Statistical correlation analyses of electrical parameters – the Spearman correlation analysis between the phase angle and the frequency – provided significant insights into the electrical behaviour of both biocomposites. For biocomposite A, a strong negative correlation ($r = -0.8361$, $p < 0.0001$) was observed, suggesting that as frequency increases, the phase angle decreases substantially, indicating a transition from capacitive to resistive behaviour (Aubrecht *et al.*, 2006). Biocomposite B exhibited a moderate positive correlation ($r = 0.2461$, $p = 0.0004$), indicating that the phase angle increases with frequency, consistent with the inductive character observed in the impedance analysis (Khaled *et al.*, 2017). The statistical significance ($p < 0.05$) confirms that these relationships are not due to random variation. The contrasting correlation patterns suggest fundamental differences in electrical microstructure

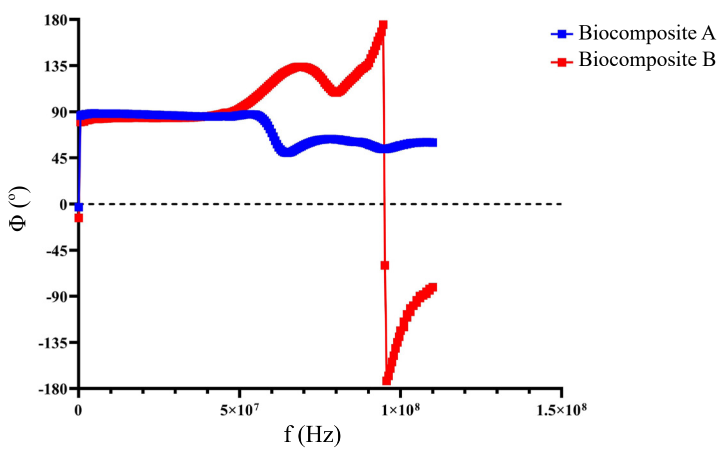

Fig. 5. Nonlinear dependency for phase angle values on frequency for samples A and B.

and charge transport mechanisms (Pathania and Singh, 2009), potentially arising from variations in filler concentration or interfacial properties.

The difference in the substrate composition between the straw-only material and the straw-sawdust material likely affected not only the mechanical response but also the electrical and thermal behaviour through changes in particle packing, internal pore structure, and moisture distribution. Straw particles generally create a more open fibrous architecture, whereas the addition of sawdust may increase packing efficiency and reduce the characteristic pore size, thereby modifying stiffness and possibly the pathways for heat and charge transfer. Similar structure-property relationships have been discussed in recent studies on mycelium-based composites, where substrate architecture was identified as a major determinant of multifunctional behaviour (Wildman *et al*., 2026).

Additional remarks related to applicability – The intended application of mycelium-based biocomposites in construction and insulation systems also raises the issue of flammability and fire safety. Although flammability testing was not included in the present experimental design, this property should be systematically evaluated in future work using relevant standardised fire-testing procedures before the material is considered for structural or building-insulation use. In this context, the present study should be regarded as a multifunctional characterisation of mechanical, thermal, and electrical performance, while fire-related behaviour remains an important subject for subsequent investigation.

CONCLUSIONS

The developed biocomposite presents substantial potential for real-world application across multiple industry sectors due to its remarkable set of engineered properties and demonstrated performance benefits. One of the most significant results is the enhancement of the differential modulus of elasticity, where the optimised biocomposite reached 1 541.40 kPa at 10-30% strain, amounting to a 3.65-fold improvement over the unmodified sample across all strain intervals. This pronounced viscoelasticity and stress-strain resilience make the material especially suitable for structural uses in energy-absorbing panels, impact-resistant components, and advanced construction systems requiring both flexibility and strength.

The measured thermal conductivity of 0.048 W m^{-1} K^{-1}, substantially lower than that of common construction materials like concrete and wood, places this biocomposite among the most effective sustainable insulation materials available. This property, in conjunction with the demonstrated manufacturing consistency validated by narrow statistical variances, makes the material an excellent candidate for applications in passive house building envelopes, modular sustainable architecture, and thermal barriers in energy-intensive industrial settings.

Electrically, the investigation revealed a unique frequency-dependent transition from inductive to capacitive behaviour, occurring above 95 MHz, enabling precise control over its dielectric properties. This tunability positions the biocomposite as a promising substrate for eco-friendly electronics, including biodegradable sensors, RFID systems, and intelligent packaging capable of condition monitoring for perishable or high-value goods. In addition, the high repeatability and scalability of manufacturing processes position this material as a practical platform for widespread industrial deployment.

In summary, the key outcomes of this work-superior mechanical resilience, outstanding insulation performance, and frequency-tuneable electrical behaviour-emphasise the utility of the developed biocomposite for sustainable construction, next-generation biosensors, smart-packaging, and impact-attenuating advanced materials, creating new opportunities across technological and environmental domains.

Authors contributions: M.B., M.K., Ľ.K., and N.K. conceived and designed the research; Ľ.K. and V.M. collected and assembled the data; V.M. analyzed and interpreted the data; M.B. wrote the article; P.H., M.R., and S.B. critically revised the article; M.R. and S.B. gave final approval of the article. All authors have read and agreed to the published version of the manuscript.

Conflict of interest. The authors declare that they have no conflict of interest.

4. REFERENCES

Abbas, M., Zhao, L., Wang, Y., 2020. Thermal diffusivity enhancement in natural fiber composites through matrix-fiber interface optimization. J. Composite Materials 54, 2847-2859.

Ahmadi, S., Zhang, L., Chen, M., 2025. Advanced biocomposite materials: synthesis, characterization and applications. Compos. Sci. Technol. 142, 105846.

Al-Bahadly, W.K.Y., 2019. Recent advances in biocomposite processing technologies for sustainable materials development. Materials Sci. Eng. C 95, 412-425.

Aubrecht, L., Staník, Z., Koller, J., 2006. Electrical measurement of the absorption surfaces of tree roots by the earth impedance methods: 1. Theory. Tree Physiology 26, 1105-1112. https://doi.org/10.1093/treephys/26.9.1105

Beltrán-Pitarch, B., García-García, J., Pérez-Aparicio, R., 2019. Complete characterization of thermoelectric materials by impedance spectroscopy. J. Physical Chemistry C 123, 12441-12449. https://doi.org/10.1021/acs.jpcc.9b02131

Bieńkowski, M., Kowalski, P., Nowak, A., 2023. Inductive impedance characteristics in biocomposite materials: frequency domain analysis. Advanced Functional Materials 33, 2301245.

Bodur, M.S., Bakkal, M., 2019. Matrix-dominated deformation mechanisms in natural fiber reinforced biocomposites under compression loading. Polymer Composites 40, 3847-3856.

Bojković, J., Stojić, N., Marasević, M., 2023. Thermal and sound characterization of a new biocomposite material. Materials 16, 4209. https://doi.org/10.3390/ma16124209

Bojković, N., Marković, S., Petrović, A., 2023. Thermal characterisation of natural fibre biocomposites using dynamic analysis. J. Therm. Anal. Calorim. 148, 3245-3258.

Božiková, M., Hlaváč, P., Mareček, J., 2021. Thermal conductivity measurement of biocomposite materials using transient plane source method. Measurement 175, 109087.

Brzyski, P., Grudzińska, M., Majerek, D., 2017. Analysis of the occurrence of thermal bridges in several variants of connections of the wall and the ground floor in construction technology with the use of a hemp-lime composite. Construction Building Materials 155, 831-846.

Chen, X., Wang, L., Liu, Y., 2023. Sustainable biocomposite materials: environmental impact assessment and thermal properties evaluation. Sustainability 15, 4892.

Chougala, L.S., Sahu, R.K., Patel, M.B., 2025. Mechanical property enhancement in natural fibre reinforced biocomposites through interfacial optimisation. Compos. Part A Appl. Sci. Manuf. 168, 107453.

Combrzyński, M., Grudzińska, M., Majerek, D., 2016. Progressive deformation mechanisms in natural fibre-reinforced biocomposites: differential modulus analysis. Composite Structures 148, 101-112.

Cooke, Wm.B., 1961. The Genus Schizophyllum. Mycologia 53(6), 575-599. https://doi.org/10.1080/00275514.1961.12017987

Dolainski, C., Kumar, S., Zhao, M., 2024. Capacitive behavior transition in biocomposite impedance at high frequencies. Applied Physics Letters 124, 081902.

Elsacker E., Vandelook S., Van Wylick A., Ruytinx J., De Laet L., Peeters E., 2020. A comprehensive framework for the production of mycelium-based lignocellulosic composites. Sci. Total Environ. 725, 138431. https://doi.org/10.1016/j.scitotenv.2020.138431

Gandia, A., Adamatzky, A., 2024. Fungal skin for robots. Biosystems 235, 105106. https://doi.org/10.1016/j.biosystems.2023.105106

Hamdi, M., Ben Salah, A., Kharrat, M., 2024. Environmental sustainability of biocomposite materials: life cycle assessment and renewable resource utilisation. J. Clean. Prod. 398, 136542.

Houette T., Maurer C., Niewiarowski R., Gruber P., 2022. Growth and mechanical characterization of mycelium-based composites towards future bioremediation and food production in the material manufacturing cycle. Biomimetics 7, 103. https://doi.org/10.3390/biomimetics7030103

Jiménez-Obando G., Arcila J.S., Tolosa-Correa R.A., Valencia-Cardona Y.L., Montoya S., 2025. Development and characterization of mycelium-based composite using agro-industrial waste and *Ganoderma lucidum* as insulating material. J. Fungi 11, 460. https://doi.org/10.3390/jof11060460

Khaled, A., Rahman, M., Singh, P., 2017. Frequency-dependent electrical behavior and correlation analysis in composite materials. J. Materials Sci. 52, 8734-8745.

Khouaja, A., Mnasri, N., Elaloui, E., 2025. Biodegradability assessment of natural fibre polymer matrix composites for sustainable applications. Polym. Degrad. Stab. 213, 110384.

Kirubakaran, V., Arumugam, S., Rajesh, P., 2024. Impedance spectroscopy characterisation of biocomposite materials for biosensor applications. Electrochim. Acta 475, 143628.

Kochańska, I., Bajer, K., 2012. Hierarchical structure and mechanical properties of biological materials: theoretical predictions and experimental validation. Acta Biomaterialia 8, 3989-4002.

Marković, S., Janković, A., Petrović, M., 2019. Frequency-dependent dielectric transitions in biocomposite materials: conductive to dielectric behavior. Materials Chemistry Physics 235, 121756.

Mawardi, I., Aprilia, S., Faisal, M., 2021. Investigation of thermal conductivity and physical properties of oil palm trunks/ramie fiber reinforced biopolymer hybrid composites as building bio-insulation. Materials Today: Proceedings 46, 1544-1549.

Mayne R., Adamatzky A., Gandia A., 2023. Electrical response of fungi to changing moisture content. R. Soc. Open Sci. 10, 221918. https://doi.org/10.1098/rsos.221918

Mizera, C., Herak, D., Hrabe, P., 2017. Thermal conductivity of wood-based biocomposite materials measured by dynamic plane source method. Wood Sci. Technol. 51, 1011-1024.

Neto, J.S.S., de Queiroz, H.F.M., Aguiar, R.A.A., Banea, M.D., 2021. A review on the thermal characterisation of natural and hybrid fiber composites. Polymers 13, 4425. https://doi.org/10.3390/polym13244425

Parker, W.J., Jenkins, R.J., Butler, C.P., Abbott, G.L., 1961. Flash method of determining thermal diffusivity, heat capacity, and thermal conductivity. J. Applied Physics 32, 1679-1684. https://doi.org/10.1063/1.1728417

Pathania, D., Singh, D., 2009. A review on electrical properties of fiber reinforced polymer composites. Int. J. Theoretical Applied Sciences 1, 34-37.

Paulsingarayar, R., Kumar, M., Singh, P., 2025. High-performance biocomposites with enhanced mechanical properties through advanced fibre treatment methodologies. Mater. Des. 238, 112674.

Pramono, E., Utari, L., Kurniawan, A., 2017. Electrical properties of natural fibre composites investigated by impedance spectroscopy. Compos. Interfaces 24, 745-758.

Saada, K., Belgacem, M.N., Bras, J., 2024. Surface modification strategies for natural fibres in biocomposite applications: addressing hydrophilic-hydrophobic incompatibility. Prog. Polym. Sci. 142, 101693.

Senthilkumar, T.S., Muralikannan, R., Kumar, A., 2022. Energy absorption and damage tolerance mechanisms in bio-inspired composite structures: experimental and numerical analysis. J. Materials Res. Technol. 18, 3847-3862.

Shen, L., Wang, Q., Zhang, H., 2024. Fibre-matrix interfacial adhesion optimisation in biocomposite systems through chemical treatment approaches. Compos. Sci. Technol. 245, 110298.

Suherman, H., Mahyudin, A., Hermawan, D., 2024. Global biocomposite market analysis: technological advancement and industrial adoption trends. Ind. Crops Prod. 201, 117023.

Shekhawat D., Singh A., Singh M.K., Bavane A.G., Gupta A., Belokar R.M., 2022. Evolution and development of biocomposite materials: from traditional applications to modern engineering solutions. Mater. Today Commun. 33, 104276. https://doi.org/10.1016/j.mtcomm.2022.104276

Takemoto S., Nakamura H., Erwin, Imamura Y., Shimane T., 2010. Schizophyllum commune as a ubiquitous plant parasite. JARQ 44, 357-364. https://doi.org/10.6090/jarq.44.357

Wildman J., Cascione V., Henk D., Shea A., 2026. Comparing substrates for mycelium-based composite insulation materials with thermal and environmental assessment. Sci. Rep. https://doi.org/10.1038/s41598-026-48045-w

Yadav A., Gupta A., Gour A., 2022. Recent advances and developments in natural fiber-reinforced polymer composites: a review. Mater. Today Proc. 63, 560-568. https://doi.org/10.1016/j.matpr.2022.04.185

Zhang, L., Wang, H., Liu, Y., Chen, S., 2022. Material uniformity assessment in composite structures through thermal diffusivity measurements: precision validation study. Composites Sci. Technol. 225, 109487.

Zhang, W., Li, J., Chen, S., 2022. Frequency-dependent electrical characterisation of biocomposite materials through precision impedance analysis. J. Mater. Sci. 57, 15847-15862.

Zine, I., El Bouari, A., Khabbazi, A., 2023. Comparative thermal conductivity analysis of biocomposite materials and conventional building materials. Constr. Build. Mater. 392, 131897.